Determination of Pesticides by Gas Chromatography Combined with Mass Spectrometry Using Femtosecond Lasers Emitting at 267, 400, and 800 nm as the Ionization Source

Yang, Xixiang
Department of Applied Chemistry, Graduate School of Engineering, Kyushu University

Imasaka, Tomoko
Department of Environmental Design, Graduate School of Design, Kyushu University

Imasaka, Totaro
Division of International Strategy, Center of Future Chemistry, Kyushu University

出版情報：Analytical chemistry. 90 (7), pp.4886-4893, 2018-03-06. American Chemical Society
バージョン：
権利関係：

Determination of Pesticides by Gas Chromatography Combined with Mass Spectrometry Using Femtosecond Lasers Emitting at 267, 400, and 800 nm as the Ionization Source

Xixiang Yang,[†] * Tomoko Imasaka,[§] and Totaro Imasaka[#]

[†]*Department of Applied Chemistry, Graduate School of Engineering, Kyushu University, 744 Motooka, Nishi-ku, Fukuoka 819-0395, Japan*

[§]*Department of Environmental Design, Graduate School of Design, Kyushu University, 4-9-1, Shiobaru, Minami-ku, Fukuoka 815-8540, Japan*

[#]*Division of International Strategy, Center of Future Chemistry, Kyushu University, 744 Motooka, Nishi-ku, Fukuoka 819-0395, Japan*

* To whom correspondence should be addressed. E-mail: yang.xixiang.888@s.kyushu-u.ac.jp

ABSTRACT: A standard sample mixture containing 51 pesticides was separated by gas chromatography (GC) and the constituents were identified by mass spectrometry (MS) using femtosecond lasers emitting at 267, 400, and 800 nm as the ionization source. A two-dimensional display of the GC/MS was successfully used for the determination of these compounds. A molecular ion was observed for 38 of the compounds at 267 nm and for 30 of the compounds at 800 nm, in contrast to 27 among 50 compounds when electron ionization was used. These results suggest that the ultraviolet laser is superior to the near-infrared laser for molecular weight determinations and for a more reliable analysis of these compounds. In order to study the conditions for optimal ionization, the experimental data were examined using the spectral properties, i.e., the excitation and ionization energies and absorption spectra for the neutral and ionized species, obtained by quantum chemical calculations. A few molecules remained unexplained by the currently reported rules, requiring additional rules for developing a full understanding the femtosecond ionization process. The pesticides in the homogenized matrix obtained from kabosu (citrus sphaerocarpa) were measured using lasers emitting at 267 and 800 nm. The pesticides were clearly separated and measured on the two-dimensional display, especially for the data measured at 267 nm, suggesting that this technique would have potential for use in the practical trace analysis of the pesticides in the environment.

Pesticides have been in widespread use to increase the production rate of various crops, and their use has increased rapidly during the 20th century. Most pesticides are toxic not only to pests but also for humans. Numerous pesticides persist for a long time in the environment because they are highly stable, although some are no longer in use.[1-3] Many kinds of pesticides are widely spread in water, soil, and air. Due to their high toxicity and stability, several pesticides have been categorized as persistent organic pollutants (POPs) by the Stockholm Convention.[4,5] The concentration of pesticides in the environment is extremely low, while numerous other organic compounds are present at high concentrations.[6] In addition, many types of pesticides exist in agricultural products. Therefore, a sensitive as well as selective analytical method would be desirable for the determination of pesticides, in conjunction with a simple pretreatment procedure prior to the measurement.[7-11]

Several analytical methods are currently available for the determination of the pesticides. Liquid chromatography/mass spectrometry (LC/MS),[12,13] liquid chromatography/tandem mass spectrometry (LC/MS-MS),[14-17] and gas chromatography/mass spectrometry (GC/MS) [18,19] are the most popular analytical methods that have been reported. Recently, gas chromatography combined with multiphoton ionization time-of-flight mass spectrometry (GC/MPI/TOF-MS) using a femtosecond laser as the ionization source has been applied to the trace analysis of pesticides in an actual sample,[20,21] the technique of which provides subfemtogram detection limits for organic compounds. In contrast to other ionization methods such as electron ionization (EI), this technique can be used for soft ionization of an organic molecule, which permits a molecular ion to be observed. In addition, the background signal arising from interfering substances can be significantly decreased by using a laser with an optimal wavelength for ionization.

Since the efficiency of ionization depends on the spectral properties of the analyte molecule, it is necessary to optimize the ionization conditions, such as the laser wavelength used for the pesticides to be examined. A variety of pesticides with complex chemical structures have been developed for use against highly resistant pests, which makes it more difficult to determine the optimal conditions. In most recent studies, the optimal laser wavelength has been determined experimentally based on a trial-and-error approach. Enantiomers, in addition to several structural isomers of hexachlorocyclohexane, have recently been separated using a GC column with an optically-active stationary phase and then measured by MPI/TOF-MS.[22] In this study, a far-ultraviolet femtosecond laser emitting at 200 nm was used, and the molecular ion was more clearly observed than the case of the laser emitting at 267 nm through resonance-enhanced two-photon ionization (RE2PI), since they have strong absorption bands at 200 nm. Similar data have been reported for allergens in fragrances.[23] This approach using the laser emitting at 200 nm is useful for more reliable identification of analytes. However, the optimal laser wavelength depends on the spectral property and then the chemical structure of the molecule. In practical trace analysis, the limit of detection (LOD) is determined by the background signal arising from interfering substances in the real sample. Therefore, it would be necessary to optimize the laser wavelength for all of the pesticides to be examined.

There are two major approaches for determining the optimal wavelength for ionization. One would involve the use of an ultraviolet (UV) laser for RE2PI (especially for aromatic molecules having an absorption band in the UV region), which increases the efficiency of ionization via the singlet excited state. When a laser with a pulse width of ca. 50 fs was used in a recent study, the efficiency of non-resonant two-photon ionization (NR2PI) reached a level that was nearly identical to that of RE2PI.[24] This approach of NR2PI can reduce the excess energy in the ionization, since the photon energy, i.e., the laser wavelength, can be adjusted to a half of the ionization energy, thus suppressing fragmentation and enhancing the signal of the molecular ion. For example, this technique has been utilized for observing a molecular ion derived from triacetone triperoxide, an explosive that is frequently used in terrorist attacks.[25]

Another would be the use of a near-infrared (NIR) laser for non-resonant MPI. Although more than several photons are required for ionization, the efficiency can be improved by using a laser with a high peak power. When the molecular ion has no absorption band in the NIR region, fragmentation can be reduced and a molecular ion can be efficiently observed.[26-28] It is reported that a laser with a lower pulse energy and a shorter pulse width is preferential for observing a molecular ion and that a ring-shaped molecule is more stable against a linear molecule and is resistive against the fragmentation.[23,24,29-31] In addition, a linearly-polarized beam has been reported to be more useful to reduce the fragmentation against the circularly-polarized beam.[32] However, many types of pesticides have complicated chemical structures, and their ionization mechanisms have not yet been studied in detail. Thus, a guideline for observing a molecular ion should be examined at different wavelengths in order to achieve optimal ionization, which would also provide useful information regarding the mechanism for the ionization of a pesticide.

In this study, we measured two-dimensional displays against the retention time in GC and the mass/charge ratio (*m/z*) in MS for a sample mixture containing 51 pesticides and calculated the LODs using femtosecond lasers emitting at 267, 400, and 800 nm as the ionization source in MS. The optimal wavelength for suppressing fragmentation was examined, and the results are discussed based on spectral properties obtained by quantum chemical calculations to clarify the ionization mechanism. We also studied some exceptional cases for which additional rules were required to explain unexpected data. The present analytical technique was applied to the determination of pesticides in homogenized matrices derived from actual samples, and the results suggest that this technique has potential advantages for use in the trace analysis of the pesticides in agriculture products.

EXPERIMENTAL SECTION

Apparatus. The experimental apparatus used in the study was a combination of a commercially available GC instrument and a TOF-MS developed in this laboratory. Briefly, a GC (6890N, Agilent Technologies, Santa Clara, CA, USA) equipped with an auto injector (7683B, Agilent Technologies)

was combined with a TOF-MS (HGK-1) that is commercially available from Hikari-GK, Fukuoka, Japan. The fundamental beam of a Ti:sapphire laser (800 nm, 1 kHz, 4 mJ, Elite, Coherent Co., Santa Clara, CA, USA) was converted into the second and third harmonic emissions and was used as the ionization source. The pulse energy available in this study was 220, 100, and 75 μJ at 800, 400, and 267 nm, the pulse width being 35, 37, and 62 fs at these wavelengths, respectively.

The analytes were separated using an HP-5 column (a length of 30 m, a 0.25-mm inner diameter, a 0.25-μm film thickness). The temperature program of the GC oven was as follows: initial temperature 70 °C held for 2 min, a rate of 20 °C/min to 150 °C, then 3 °C/min to 200 °C, followed by 8 °C/min to 280 °C and a hold of 10 min. The temperatures of the GC inlet port and of the transfer line between GC and MS were adjusted to 250 and 280 °C, respectively. The flow rate of helium, used as the carrier gas, was 1 mL/min. A 1-μL aliquot of sample solution was injected into the GC system.

The pesticides in the molecular beam were ionized by focusing the femtosecond laser beam. The ions induced by 2PI/MPI were accelerated toward a flight tube and were detected by microchannel plates (F4655-11, Hamamatsu Photonics, Shizuoka, Japan). The signal was recorded using a digitizer (Acqiris AP240, Agilent Technologies), and the data were analyzed using a home-made software programed by Visual Basic. The two-dimensional GC/MS display was constructed using the ORIGIN software. The color scale in the picture was slightly modified to compensate for changes in the background and sensitivity using the LabVIEW software.

Reagents. A standard sample mixture containing 51 pesticides listed in Table 1 was purchased from Hayashi Pure Chemical Ind., Ltd, Osaka, Japan, the concentration of which was 20 μg/mL for each component. This solution was diluted 10 fold (2 ng/μL) with acetone (analytical grade) supplied from Wako Pure Chemical Industries, Osaka, Japan.

Pretreatment Procedure. A fruit (kabosu) and two vegetables (cucumber and pumpkin) that were examined in this study were purchased from a local supermarket in Fukuoka. The pretreatment procedure was as follows. The sample (20 g) in a tall 300-mL beaker was mixed with 100-mL of a 4:1 mixture of acetonitrile and water and was homogenized for 2 min. The solution was then passed through a glass-fiber filter (Advantec Toyo Kaisha, Ltd., Tokyo, Japan) to remove the fiber-like substances and was transferred to a separatory funnel (200 mL). After adding NaCl (10 g) and phosphate buffer (1 M, pH 7, 2 mL), the solution was horizontally shaken for 5 min. After phase separation, the acetonitrile layer was removed by a pipette and was then passed through a column containing anhydrous Na_2SO_4 (10 g). The solvent was removed by evaporation under reduced pressure at 40 °C using a rotary evaporator.

A 2-mL solution comprised of a 3:1 mixture of acetonitrile and toluene was added to the residue and the resulting solution was loaded onto a mini-column (ENVI-Carb/NH2, 400 mg/500 mg, 6 mL, Supelco, Bellefonte, PA, USA) conditioned using a 10-mL portion of the solvent mixture. The

glassware was rinsed with a 2-mL portion of the same mixture of acetonitrile and toluene and was loaded onto the mini-column. This procedure was repeated three times.

The analyte was eluted using the same solvent mixture (12 mL). The eluent was concentrated under reduced pressure in the rotary evaporator, and the residue was dissolved with acetone, transferred to a centrifuge tube, and was gently dried under a nitrogen gas flow. The residue was dissolved with acetone (1 mL) again and was used as a sample for GC analysis. Occasionally, the standard sample mixture of pesticides (2 ng/μL for each) was added to the above solution, the final concentration being 20 pg/μL for each. The solution was stored in a refrigerator prior to the GC measurements.

Computational Methods. Quantum chemical calculations involved the use of the Gaussian 09 program series package,[33] in an attempt to develop a better understanding of the ionization mechanism for the pesticides. Minimum geometries were obtained using the B3LYP method, based on density functional theory (DFT) with a cc-pVDZ basis set.[34,35] The harmonic frequencies were calculated in order to ensure an optimum geometry providing a global energy minimum. A vertical ionization energy was evaluated from the energy difference between the ground and ionic states. The lowest eighty singlet transition energies and the oscillator strengths were calculated using time-dependent DFT (TD-DFT),[36] and the predicted absorption spectra for a neutral species and a molecular ion were obtained by assuming a Gaussian profile with a half width at half maximum of 0.333 eV for each transition.

RESULTS AND DISCUSSION

Two-Dimensional Display and Limits of Detection. A two-dimensional display measured at 267 nm for a standard sample mixture containing 51 pesticides is shown in Figure 1. Numerous signals were observed in the display. The total ion chromatogram shown at the top of the figure suggests complete separation of the components by GC. The mass spectrum can be extracted from the data measured at the retention time, at which a specific pesticide listed in Table 1 appears. A molecular ion was clearly observed as a major peak for many pesticides. As shown in the expanded view, a series of isotopomers, i.e., $[M]^+$, $[M+1]^+$, and $[M+2]^+$, which contains zero, one, or two ^{13}C atoms in a molecule, was observed for flutolanil (20). The fragment ions can also be assigned from the *m/z* values. These results suggest that the separation and resolution of the GC and MS are sufficient for these samples and that the method is applicable to these types of analyses. It should be noted that, in most cases, the pesticides in the sample contain aromatic rings as shown in Figure S-1 and, therefore, can be efficiently ionized through RE2PI.

A two-dimensional display measured at 400 nm is shown in Figure 2. As shown in the expanded view, molecular ions for alachlor (10) and isoprothioane (21) can be clearly observed. The data measured at 800 nm are shown in Figure 3. As shown in the insert, an $[M+2]^+$ signal is more clearly observed for dimethipin (5) than molinate (1), due to the larger number of sulfur atoms in the molecule;

there are two major isotopes for sulfur, i.e., ^{32}S and ^{34}S. Although many signal peaks were observed, due to the larger pulse energy of the laser at longer wavelengths, the intensities of the signals, especially for high *m/z* values, would be relatively low. These results suggest that fragmentation is more efficient when the visible (VIS) and near-infrared (NIR) lasers were used.

Table 1 shows the LODs for the pesticides measured at 267, 400, and 800 nm using the signals arising from molecular and fragment ions. Molecular ions were observed for 38 pesticides at 267 nm, which is in contrast to 30 pesticides at 400 and 800 nm. On the other hand, the fragment ions were observed as major signals for 45 and 46 compounds at 400 and 800 nm, respectively, which is slightly larger than the value of 43 at 267 nm. As a rule of thumb, a laser emitting at 267 nm appears to be slightly better for observing a molecular ion than the laser emitting at 400 and 800 nm. The lowest LODs among the three data sets measured at the different wavelengths are marked in Table 1. Compounds that elute earlier (smaller and nonpolar compounds) appear to be preferentially ionized at 800 nm. Only a limited number of compounds appear to be ionized efficiently at 400 nm. On the other hand, compounds that elute later (larger and polar compounds) are more extensively ionized at 267 nm.

Optimum Wavelength for Ionization. Absorption spectra were calculated for all the pesticides in both neutral and ionic forms, in addition to other spectral parameters, including excitation and ionization energies based on quantum chemical calculation. The results are shown in Figure S-2, which were used for studies related to the ionization mechanism in the following subsections, where the pesticides were tentatively grouped into five categories (Groups A- E). Table 1 modified according to this grouping is shown in Table S-2.

Optimum both at 267 and 800 nm (Group A). When the neutral form of the pesticide has an absorption band at 267 nm and an ionization energy lower than the sum of the energies of two photons, the molecule can be ionized through efficient RE2PI. In addition, when the molecular ion has no absorption band at 800 nm, the molecule can be ionized through MPI with a minimum excess energy and remains as a molecular ion, since it does not absorb additional photons for dissociation. In this case, the pesticide molecule would be predicted to be efficiently ionized and provide a molecular ion, the value for the LOD being low both at 267 and 800 nm. Flutolanil (20) represents a typical compound of this group (see Figure S-3). This molecule can be efficiently ionized, and the LODs shown in Table 1 were found to be 11 and 6.4 pg/μL at 267 and 800 nm, respectively. Clomeprop (35) represents a similar example (16 pg/μL at 267 nm and 12 pg/μL at 800 nm). These aromatic molecules have low LODs at 267 nm, due to small excess energies in RE2PI. It has been reported that fragmentation is minimal when the excess energy is ≤ 1 eV and was more significant when >3 eV.[24] The situation is nearly identical for aromatic molecules such as quinoclamine (13) and non-aromatic molecules such as isoprothiolane (21) as well. Other molecules such as cyhalofop-butyl (36), chlorpropham (2), buprofezin (26), benfluralin (3), bifenox (34), and chlorefenson (19) can also be classified in this category.

Although other molecules such as acrinathrin (39), halfenprox (43), flucythrinate (44/45), fenvalerate (46), fluvalinate (47/48), bifenthrin (32), and cyfluthrin (42) have reasonable LODs in the ionization at 267 nm, it was more difficult to detect them by ionization at 800 nm in MS, even though the molecular ions had either no or a small absorption band at 800 nm in the calculated absorption spectrum. It is, at present, difficult to explain the above findings with confidence. However, these molecules have strong absorption bands in the region above 1000 nm, suggesting a considerable degree of molar absorptivity in the actual absorption spectrum, due to high vibrational levels on the excited electronic state of the molecular ion, since these molecules have a long/large side chain and then numerous low-frequency vibrational modes (see the chemical structures shown in Figure S-1). Note that the spectrum was calculated by assuming a spectral bandwidth of 0.333 eV for all the electronic transitions (see the section of Computational Methods) and by neglecting the Franck Condon factors for individual vibrational modes. Accordingly, the molecular ion would actually absorb the photons at 800 nm, which then undergoes dissociation to form fragments.

Optimum at 267 nm but not at 800 nm (Group B). Fluquinconazole (40) has an absorption band at 267 nm (3.92×10^4 $M^{-1}cm^{-1}$), and the molecular ion has an absorption band at 800 nm (0.25×10^4 $M^{-1}cm^{-1}$). The LOD was determined to be 8.2 pg/μL at 267 nm, which is lower than the value (470 pg/μL) obtained at 800 nm. The LODs observed using the fragment ions were 6.8 pg/μL at 267 nm and 15 pg/μL at 800 nm. Then, the poor LOD observed at 800 nm using the molecular ion can be attributed to the absorption of an additional NIR photon from the ionized state to form fragments. It should also be noted that only fragment ions were observed in EI-MS, as shown in the figures cited in Table S-1. On the other hand, a molecular ion can be observed by optimizing the laser wavelength in photoionization, suggesting that the present technique has a distinct advantage over EI-MS and would be useful for more reliable analyses and for reducing background arising from interfering substances in the sample. Other molecules such as fenpropathrin (33), azoxystrobin (51), kresoxim methyl (27) can be classified in this category.

As expected, it was difficult to determine chlorfenapyr (30), bromopropylate (31), deltamethrin (50), and cyflufenamid (29) using the laser emitting at 800 nm. However, it was also difficult to measure these compounds even using the laser emitting at 267 nm, although they have absorption bands in this spectral region. These exceptions are likely due to the presence of bromine atoms and a cyclopropyl group in the molecule, which are dissociative or reactive and form small fragments.

Optimum at 800 nm but not at 267 nm (Group C). Molinate (1) has no absorption band both at 267 and 800 nm and is a typical example of this category. As expected, it had a low LOD value (1.41 pg/μL) when the laser emitting at 800 nm was employed. On the other hand, the LOD value was moderate (36 pg/μL) at 267 nm. This suggests that using the laser emitting at 800 nm is advisable when the molecular ion has no absorption band at the laser wavelength. A similar situation was observed for atrazine (6) and cyanazine (14), both of which provided low LODs at 800 nm and low/moderate LODs at 267 nm. These data suggest that the molecules can be efficiently ionized

through NR2PI when a high-intensity laser with a pulse width less than 50 fs is used, as reported previously.[24] Fenarimol (37) and bromobutide (8) can also be classified in this category.

Not optimum both at 267 and 800 nm (Group D). Dithiopyr (12) has no or a small absorption band at 267 nm, and the molecular ion has an absorption band at around 800 nm. For this reason, it was difficult to detect the molecular ion at a concentration of 20 pg/μL. Other compounds such as fenchlorphos (11), bromophos methyl (16), in addition to pyrazophos (38) with a bulky side chain, DEF (tribufos) (22) with long chains, and alachlor (10) with flexible chains, have rather poor LODs, as expected. Fragmentation would be accelerated by associating with the low frequency modes of the bully/long/flexible side chain, the trend of which has been reported in the reference.[23]

Miscellaneous molecules (Group E). There are several compounds that cannot be explained from the rules described above. For example, dichloran (4) is a simple molecule with no long/flexible side chain and has a strong absorption band at 267 nm (3.9×10^3 $M^{-1}cm^{-1}$) and a small excess energy (0.8 eV) in RE2PI at 267 nm. It is, however, difficult to observe any signal at the concentration of 20 pg/μL. In addition, the molecular ion has no absorption band at around 800 nm and is predicted to remain as a molecular ion in MS. However, only fragment ions can be observed, when the molecules are ionized at 800 nm. In EI-MS, a molecular ion can be observed, although the fragment ions are observed as major ions. This is the only case where a molecular ion can be observed not in 2PI/MPI-MS but in EI-MS. No reasonable explanation can be provided in this study, requiring further investigation to clarify these phenomena. However, it is well known that this molecule can form an intra-molecular charge-transfer complex due to $–NH_2$ and NO_2 functional groups combined at the para-position of the aromatic ring, which would play an important role in the photoionization process. Similar results have been observed for an intra-molecular charge-transfer molecule of *p*-nitroaniline, in which fragmentation has been reported to be more significant at higher pulse energies (0.1→0.6 mJ) and longer pulse widths (0.1→5 ps) at 790 nm.[37]

Other molecules that are difficult to explain are the *α*- and *β*-endosulfan isomers (18) (28). The retention times are very different from each other due to the different chemical structures of the isomers (*cf.* Figure S-1) and then their different physical properties such as polarity that determines the melting point (*α* isomer, 109.28 ºC; *β* isomer, 213.28 ºC). The spectral properties of the molecules are, however, very similar as shown in Figure S-2, and these molecules would be expected to be ionized through NR2PI at 267 nm. It should be noted that measuring *α*-endosulfan was difficult by ionizations at 267 and 800 nm, which is in contrast to *β*-endosulfan (the LODs are 11.8 and 70 pg/μL at 267 and 800 nm, respectively) (see the insert of Figure 1). Note that the major ion observed at 267 nm was a molecular ion. On the other hand, no significant difference is observed between *α*- and *β*-endosulfans in the mass spectrum obtained by EI, although the intensities of the molecular ions are much smaller than those of the fragment ions.

Other interesting compounds include molecules that contain a functional group of 1,2,4-triazole, i.e., azaconazole (25), difenoconazole (49), dicrobutrazole (23), and cafenstrole (41). It is difficult

even to measure these compounds, although they have a small leading-edge absorption band at the longer wavelength side of the absorption spectrum at around 267 nm and the molecular ion does not have a strong absorption band at around 800 nm. Other molecules that can be grouped in this category would be simeconazole (9), fipronil (17), and myclobutanil (24). These molecules seldom provide a molecular ion in EI-MS. It should be noted that these molecules all contain a strained functional group or a flexible/bulky side chain. It would be predicted that this type of molecule would be more difficult to detect, due to a large distortion and the small barrier for dissociation. Note that fluquinconazole (40), with no side chain, provides a molecular ion when ionized at 267 nm (see Section 2.2).

There are a few other exceptional cases, which cannot be explained by the rules described above. For example, fthalide (15) and triallate (7) have a strong absorption band at around 267 nm but the LOD values were poor (830 pg/μL and ND). On the other hand, the LOD calculated from the signal of a molecule ion was very low for dimethipin (5) (4 pg/μL) at 800 nm (see Section 1 and Figure 3), although it has a strong absorption band at 800 nm for the molecular ion. Thus, finding the optimum ionization condition based on the two schemes, *i.e.*, efficient UV-RE2PI and fragmentation by NIR-MPI, using the data obtained by the computational method is sometimes difficult for several pesticides. Then, further investigations will be necessary for arriving at a coherent explanation for these compounds.

Pesticides in Actual Sample. In this study, samples extracted from a fruit (kabosu) and vegetables (cucumber and pumpkin) were measured at 267 and 800 nm. A two-dimensional display obtained for the sample extracted from kabosu and measured at 267 nm is shown in Figure 4 (a). Numerous signal spots appeared in the data. However, none of the signals could be assigned to the pesticides examined in this study. The same findings were obtained for the vegetable samples. These results suggest that fruit and vegetables obtained in a supermarket are not contaminated by the pesticides. To study validity of the method, the standard mixture of pesticides was added to the solution extracted from the actual samples. Many additional signals appeared in the two-dimensional display, in addition to signals arising from contaminants, as shown in Figure 4 (b). These signals can be assigned to the pesticides by comparing the data with those obtained in Figure 1. The same samples were also measured using the laser emitting at 800 nm. A pattern similar to that shown in Figure 4 was observed in the two-dimensional display, as shown in Figure 5. A careful examination of the data shown in Figures 4 and 5 indicated that the larger ions such as the molecular ions derived from the pesticides with higher molecular weights, which elute later in GC, were more pronounced when the laser emitting at 267 nm was used (see the area specified by a tilted elliptical circle with a broken line). This result suggests that RE2PI at 267 nm is superior to MPI at 800 nm for more sensitive as well as reliable determination of the pesticides.

CONCLUSIONS

The two-dimensional display was obtained for a sample mixture containing 51 pesticides, and the LODs obtained at 267, 400, and 800 nm were compared. The findings indicate that MS measured at 267 nm was slightly more sensitive than MS measured at 400 and 800 nm, although the results depended on the pesticides examined. The data were evaluated using spectral properties obtained by quantum chemical calculations. As a rule of thumb, when a molecule has an absorption band at 267 nm, a laser emitting at 267 nm can be successfully used for efficient ionization through RE2PI and for observing a molecular ion. Note that the efficiency of NR2PI becomes nearly comparable to that of RE2PI when the laser pulse width was reduced to ca. 50 fs. When a molecular ion shows no or a small absorption band at 800 nm, a laser emitting at 800 nm can be preferentially used for observing a molecular ion and provides a low LOD. In addition, a strained functional group or a bulky/long/flexible side chain accelerates the degree of fragmentation.

There were several exceptional cases for which it was difficult to explain using the above rules. For example, dichloran (4), which forms an intramolecular charge-transfer complex, was difficult to detect both at 267 and 800 nm, even though it has a strong absorption band at 267 nm and the molecular ion has no absorption band at 800 nm. It is interesting to note that α- and *β*-endosulfan (18, 28) have nearly the same spectral properties, *e.g.*, spectral shape, molar absorptivity, ionization energy, *etc.*, for both neutral and ionic species but the former was difficult to detect but the latter was easily detected by photoionization MS.

Selectivity in photoionization can be tuned by changing the laser wavelength, which is preferential for enhancing an analyte signal and for suppressing background arising from interfering substances. This favorable effect can reduce the time required for sample pretreatment, thus reducing the cost of an analysis. Moreover, the data obtained at different wavelengths can be used to narrow down the candidate compounds that remain unassigned in a comprehensive analysis by GC/MS. In order to demonstrate the potential advantage of the methodology, GC/MPI/TOF-MS was used to analyze pesticides in some typical foods. In fact, the pesticides in homogenized matrix obtained from kabosu were separated and measured on a two-dimensional display, suggesting that this technique has potential for use as a new tool for practical trace analyses of pesticides in the environment.

ACKNOWLEDGMENTS

This research was supported by a Grant-in-Aid for Scientific Research from the Japan Society for the Promotion of Science [JSPS KAKENHI Grant Numbers JP26220806 and JP15K01227]. Quantum chemical calculations were mainly carried out using the computer facilities at the Research Institute for Information Technology, Kyushu University. The authors greatly appreciate Koji Takahashi and Hiroko Tsukatani of the Fukuoka Institute of Health and Environmental Sciences for their gifts of the actual samples prepared in their institution.

REFERENCES

(1) Barrek, S.; Cren-Olivé, C.; Wiest, L.; Baudot, R.; Arnaudguilhem, C.; Grenier-Loustalot, M. F. *Talanta* **2009**, *79*, 712–722.

(2) Bernardi, G.; Kemmerich, M.; Ribeiro, L. C.; Adaime, M. B.; Zanella, R.; Prestes, O. D. *Talanta* **2016**, *161*, 40–47.

(3) Domínguez, I.; Romero-González, R.; Javier Arrebola Liébanas, F.; Martínez Vidal, J. L.; Garrido Frenich, A. *Trends Environ. Anal. Chem.* **2016**, *12*, 1–12.

(4) Xu, W.; Wang, X.; Cai, Z. *Anal. Chim. Acta* **2013**, *790*, 1–13.

(5) Muir, D.; Lohmann, R. *Trends Anal. Chem.* **2013**, *46*, 162–172.

(6) Kosikowska, M.; Biziuk, M. *Trends Anal. Chem.* **2010**, *29*, 1064–1072.

(7) Li, N.; Chen, J.; Shi, Y. *Talanta* **2015**, *141*, 212–219.

(8) Bresin, B.; Piol, M.; Fabbro, D.; Mancini, M. A.; Casetta, B.; Bianco, C. D. *J. Chromatogr. A* **2015**, *1376*, 167–171.

(9) Costa, A. I. G.; Queiroz, M. E. L. R.; Neves, A. A.; De Sousa, F. A.; Zambolim, L. *Food Chem.* **2015**, *181*, 64–71.

(10) Farajzadeh, M. A.; Feriduni, B.; Mogaddam, M. R. A. *Anal. Chim. Acta* **2015**, *885*, 122–131.

(11) Ali, M.; Khoshmaram, L.; Nabil, A. A. A. *J. Food Compos. Anal.* **2014**, *34*, 128–135.

(12) Rickes, S.; Cesar, P.; José, L.; Carla, G.; Clasen, F. *Food Chem.* **2017**, *220*, 510–516.

(13) Region, V.; Coscollà, C.; Hart, E.; Pastor, A.; Yusà, V. *Atmos. Environ.* **2013**, *77*, 394–403.

(14) Machado, I.; Gérez, N.; Pistón, M.; Heinzen, H.; Verónica, M. *Food Chem.* **2017**, *227*, 227–236.

(15) Nortes-Méndez, R.; Robles-Molina, J.; López-Blanco, R.; Vass, A.; Molina-Díaz, A.; Garcia-Reyes, J. F. *Talanta* **2016**, *158*, 222–228.

(16) Timofeeva, I.; Shishov, A.; Kanashina, D.; Dzema, D.; Bulatov, A. *Talanta* **2017**, *167*, 761–767.

(17) Alves, J.; Maria, J.; Ferreira, S.; Talamini, V.; Fátima, J.D; Medianeira, T.; Damian, O.; Bohrer M.; Zanella, R.; Beatriz, C.; Bottoli, G. *Food Chem.* **2016**, *213*, 616–624.

(18) Hart, E.; Coscollà, C.; Pastor, A.; Yusà, V. *Atmos. Environ.* **2012**, *62*, 118–129.

(19) Huo, F.; Tang, H.; Wu, X.; Chen, D.; Zhao, T.; Liu, P.; Li, L. *J. Chromatogr. B* **2016**, *1023–1024*, 44–54.

(20) Hashiguchi, Y.; Zaitsu, S.; Imasaka, T. *Anal. Bioanal. Chem.* **2013**, *405*, 7053–7059.

(21) Li, A.; Imasaka, T.; Uchimura, T.; Imasaka, T. *Anal. Chim. Acta* **2011**, *701*, 52–59.

(22) Yang, X.; Imasaka, T.; Li, A.; Imasaka, T. *J. Am. Soc. Mass Spectrom.* **2016**, *27*, 1999–2005.

(23) Shibuta, S.; Imasaka, T.; Imasaka, T. *Anal. Chem.* **2016**, *88*, 10693–10700.

(24) Kouno, H.; Imasaka, T. *Analyst* **2016**, *141*, 5274–5280.

(25) Hamachi, A.; Okuno, T.; Imasaka, T.; Kida, Y.; Imasaka, T. *Anal. Chem.* **2015**, *87*, 3027–3031.

(26) Yatsuhashi, T.; Nakashima, N. *J. Photochem. Photobiol. C: Photochem. Rev.* **2007**, https://doi.org/10.1016/j.jphotochemrev.2017.12.001

(27) Konar, A.; Shu, Y.; Lozovoy, V.; Jackson, J.; Levine, B.; Dantus, M. *J. Phys. Chem. A* **2014**, *118*, 11433–11450.

(28) Li, A.; Thang, D. P.; Imasaka, T.; Imasaka, T. *Analyst* **2017**, *142*, 3942–3947.

(29) Markevitch, A. N.; Smith, S. M.; Romanov, D. A.; Schlegel, H. B.; Ivanov, M. Y.; Levis, R. J. *Phys. Rev. A* **2003**, *68*, 011402.

(30) Tanaka, M.; Panja, S.; Murakami, M.; Yatsuhashi, T.; Nakashima, N. *Chem. Phys. Lett.* **2006**, *427*, 255–258.

(31) Lezius, M.; Blanchet, V.; Ivanov, M. Y.; Stolow, A. *J. Chem. Phys.* **2002**, *117*, 1575–1588.

(32) Murakami, M.; Tanaka, M.; Yatsuhashi, T.; Nakashima, N. *J. Chem. Phys*. **2007**, *126*, 104304.

(33) Frisch, M. J.; Trucks, G. W.; Schlegel, H. B.; Scuseria, G. E.; Robb, M. A.; Cheeseman, J. R.; Scalmani, G.; Barone, V.; Mennucci, B.; Petersson, G. A.; Nakatsuji, H.; Caricato, M.; Li, X.; Hratchian, H. P.; Izmaylov, A. F.; Bloino, J.; Zheng, G.; Sonnenberg, J. L.; Hada, M.; Ehara, M.; Toyota, K.; Fukuda, R.; Hasegawa, J.; Ishida, M.; Nakajima, T.; Honda, Y.; Kitao, O.; Nakai, H.; Vreven, T.; Montgomery, J. A., Jr.; Peralta, J. E.; Ogliaro, F.; Bearpark, M.; Heyd, J. J.; Brothers, E.; K. N. Kudin,; Staroverov, V. N.; Kobayashi, R.; Normand, J.; Raghavachari, K.; Rendell, A.; Burant, J. C.; Iyengar, S. S.; Tomasi, J.; Cossi, M.; Rega, N.; Millam, J. M.; Klene, M.; Knox, J. E.; Cross, J. B.; Bakken, V.; Adamo, C.; Jaramillo, J.; Gomperts, R.; Stratmann, R. E.; Yazyev, O.; Austin, A. J.; Cammi, R.; Pomelli, C.; Ochterski, J. W.; Martin, R. L.; Morokuma, K.; Zakrzewski, V. G.; Voth, G. A.; Salvador, P.; Dannenberg, J. J.; Dapprich, S.; Daniels, A. D.; Farkas, O.; Foresman, J. B.; Ortiz, J. V.; Cioslowski, J.; Fox, D. J. *Gaussian 09*, revision D.01; Gaussian Inc.: Wallingford, CT, **2009**.

(34) Becke, A. D. *J. Chem. Phys.* **1993**, *98*, 5648–5652.

(35) Dunning, Jr. T. H. *J. Chem. Phys. Lett.* **1989**, *90*, 1007–1023.

(36) Bauernschmitt, R.; Ahlrichs, R. *Chem. Phys. Lett.* **1996**, *256*, 454–464.

(37) Moore, N. P.; Menkir, G. M.; Markevitch, A. N.; Graham, P.; Levis, R. J. In *Laser Control and Manipulation of Molecules*; Bandrauk, A. D.; Fujimura, Y.; Gordon, R. J., Ed.; American Chemical Society: Washington, DC, 2002; pp 207–220.

Table 1. Limit of Detections (LODs) Obtained Using GC/MPI/TOFMS at 267, 400, and 800 nm for a Standard Sample Mixture of Pesticides.

Name of pesticide (Elution Order)	LOD at 267 nm (pg/μL)		LOD at 400 nm (pg/μL)		LOD at 800 nm (pg/μL)		Group
	M^+	F^+	M^+	F^+	M^+	F^+	
Molinate (1)	36	N.D.	5.4	6.8	1.41	2.8	C
Chlorpropham (2)	9.9	240	8.7	36	4.4	5.4	A
Benfluralin (3)	40	50	9.4	7.4	6.5	14	A
Dichloran (4)	N.D.	N.D.	N.D.	156	N.D.	82	E
Dimethipin (5)	40	40	18	34	4.4	2.2	E
Atrazine (6)	10	34	22	35	3.4	21	C
Triallate (7)	N.D.	230	380	43	78	11	E
Bromobutide (8)	189	510	67	195	31	37	C
Simeconazole (9)	N.D.	93	240	58	34	33	E
Alachlor (10)	75	88	28	35	32	27	D
Fenchlorphos (11)	N.D.	35	280	25	178	8.6	D
Dithiopyr (12)	N.D.	172	N.D.	62	N.D.	29	D
Quinoclamine (13)	29	17	6.1	3.4	3.2	15	A
Cyanazine (14)	47	280	29	56	11.2	54	C
Fthalide (15)	840	150	60	22	17	87	E
Bromophos Methyl (16)	N.D.	120	270	14	240	11.4	D
Fipronil (17)	340	54	N.D.	20	N.D.	430	E
α-Endosulfan (18)	N.D.	N.D.	N.D.	N.D.	N.D.	121	E
Chlorefenson (19)	146	96	80	36	40	26	A
Flutolanil (20)	11	5.8	5.8	5.9	6.4	11.7	A
Isoprothiolane (21)	7.2	31	4.5	38	9.8	54	A
DEF (Tribufos) (22)	78	260	58	49	48	25	D
Dicrobutrazole (23)	N.D.	N.D.	N.D.	N.D.	N.D.	N.D.	E
Myclobutanil (24)	200	220	149	30	44	18	E
Azaconazole (25)	N.D.	N.D.	N.D.	N.D.	N.D.	N.D.	E
Buprofezin (26)	22	65	15	25	22	7.1	A
Kresoxim methyl (27)	38	57	37	25	20	15	B
β-Endosulfan (28)	11.8	160	60	174	70	58	E
Cyflufenamid (29)	N.D.	N.D.	N.D.	N.D.	N.D.	N.D.	B
Chlorfenapyr (30)	N.D.	N.D.	N.D.	N.D.	N.D.	N.D.	B
Bromopropylate (31)	290	24	N.D.	16	N.D.	21	B
Bifenthrin (32)	106	15	N.D.	9.0	N.D.	3.6	A
Fenpropathrin (33)	12.7	63	51	84	72	37	B
Bifenox (34)	67	96	30	91	18	380	A
Clomeprop (35)	16	88	15	42	12	14	A
Cyhalofop-butyl (36)	6.1	24	39	41	26	16	A
Fenarimol (37)	75	96	52	63	39	23	C
Pyrazophos (38)	N.D.	N.D.	46	62	16	18	D
Acrinathrin (39)	8.6	6.1	N.D.	N.D.	N.D.	N.D.	A
Fluquinconazole (40)	8.2	6.8	24	12.5	470	15	B
Cafenstrole (41)	350	220	N.D.	95	N.D.	30	E

Cyfluthrin 1-4 (42)	310	220	N.D.	32	N.D.	42	A
Halfenprox (43)	38	23	N.D.	23	N.D.	13	A
Flucythrinate 1 (44)	56	45	N.D.	59	N.D.	60	A
Flucythrinate 2 (45)	55	67	N.D.	59	N.D.	60	A
Fenvalerate 1-2 (46)	44	61	N.D.	90	N.D.	44	A
Fluvalinate 1 (47)	78	40	N.D.	39	N.D.	44	A
Fluvalinate 2 (48)	9.2	6.6	N.D.	39	N.D.	44	A
Difenoconazole 1-2 (49)	N.D.	5.3	N.D.	34	N.D.	71	E
Deltamethrin (50)	380	120	N.D.	51	N.D.	70	B
Azoxystrobin (51)	52	148	100	37	62	32	B

N.D., not detected. M^+, molecular ion. F^+, largest fragment ion.

Figure Captions.

Figure 1. Two-dimensional display of a standard sample mixture containing 51 pesticides measured at 267 nm. Inserts show expanded views of the regions where flutolanil (20), α-endosulfan (18), and β-endosulfan (28) appear.

Figure 2. Two-dimensional display of a standard sample mixture containing 51 pesticides measured at 400 nm. Inserts show expanded views of the regions where alachlor (10) and isoprothiolane (21) appear.

Figure 3. Two-dimensional display of a standard sample mixture containing 51 pesticides measured at 800 nm. Inserts show expanded views of the regions where molinate (1) and dimethipin (5) appear.

Figure 4. Two-dimensional display measured at 267 nm. (a) kabosu (b) kabosu and 51 pesticides. A tilted elliptical circle (broken line) is drawn as a guide line to provide a visual check of the locations of the data spots.

Figure 5. Two-dimensional display measured at 800 nm. (a) kabosu (b) kabosu and 51 pesticides. A tilted elliptical circle (broken line) is drawn as a guide line to permit a visual check of the locations of the data spots.

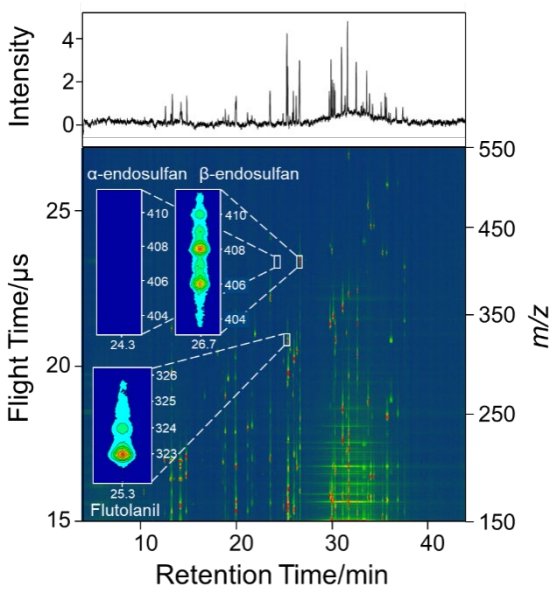

Figure 1. X. Yang et al.

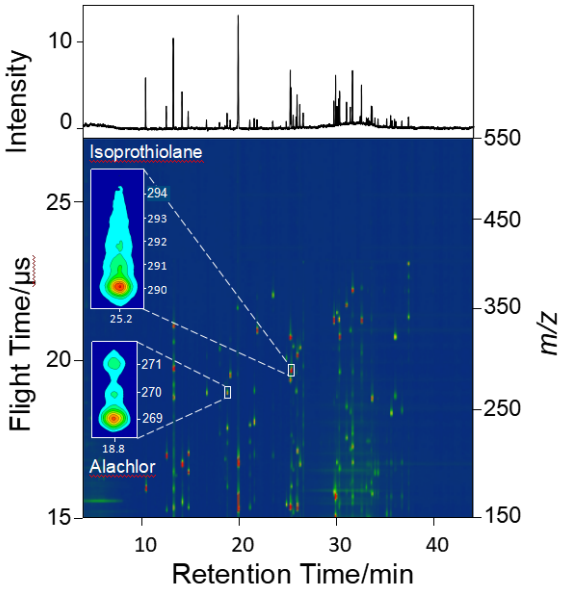

Figure 2. X. Yang et al.

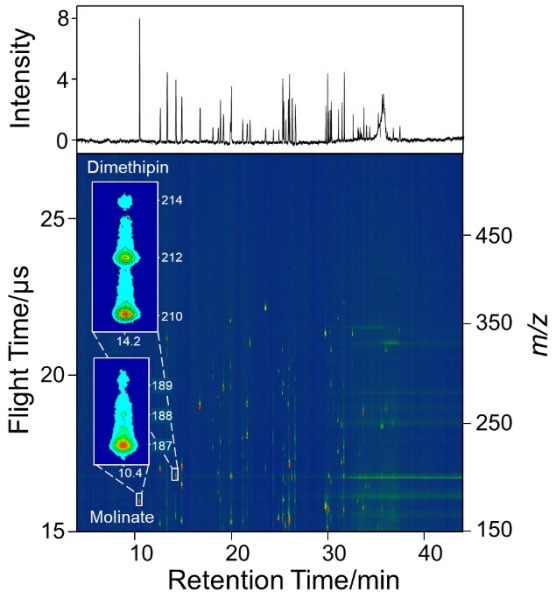

Figure 3. X. Yang et al.

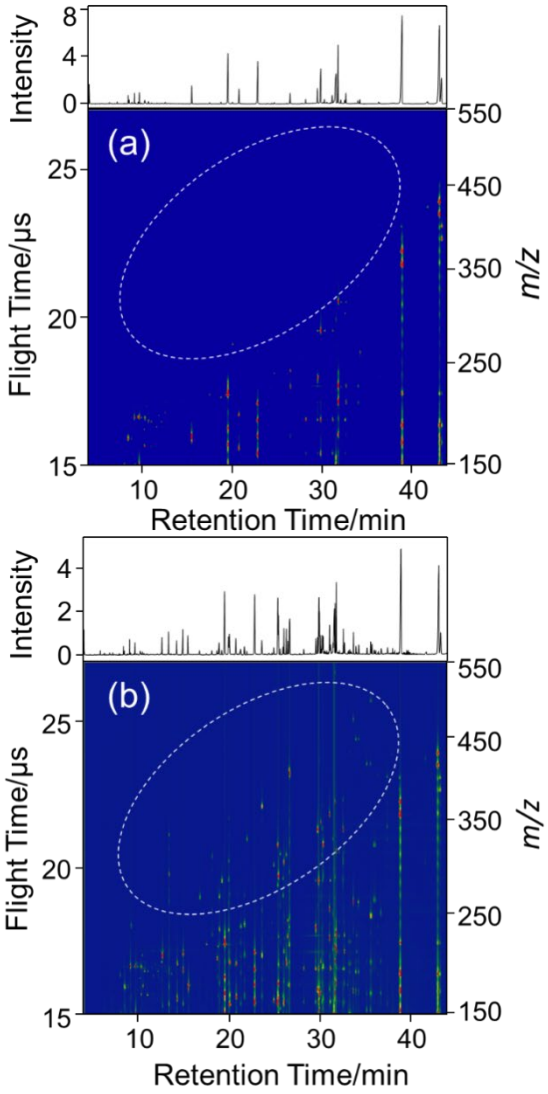

Figure 4. X. Yang et al.

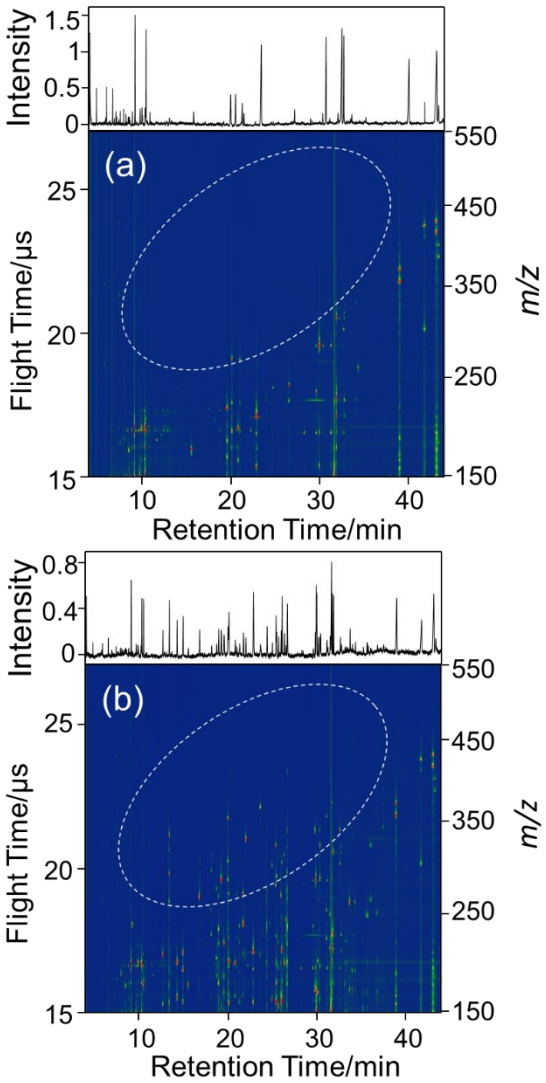

Figure 5. X. Yang et al.

For TOC only

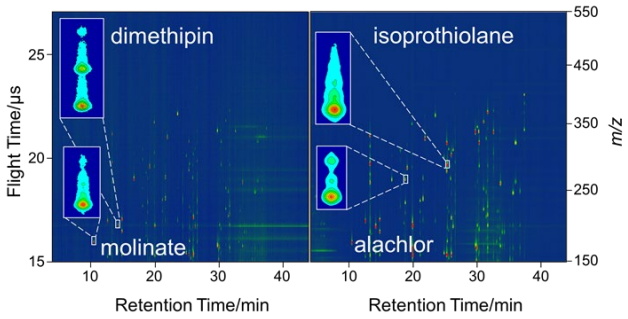
dimethipin
molinate
isoprothiolane
alachlor
Flight Time/μs
25
20
15
10
20
30
40
Retention Time/min
550
450
350
250
150
m/z